Available online at www.sciencedirect.com
ScienceDirect
Marine Chemistry 104 (2007) 186–202
MARINE CHEMISTRY
www.elsevier.com/locate/marchem

Influence of atmospheric inputs on the iron distribution in the subtropical North-East Atlantic Ocean

Géraldine Sarthou [a,*], Alex R. Baker [b], Jurjen Kramer [c], Patrick Laan [c], Agathe Laës [a,1], Simon Ussher [d], Eric P. Achterberg [e], Hein J.W. de Baar [c], Klaas R. Timmermans [c], Stéphane Blain [f]

[a] *LEMAR/UMR CNRS 6539/IUEM, Technopole Brest Iroise, F- 29280 Plouzané, France*
[b] *School of Environmental Sciences, University of East Anglia, Norwich NR4 7TJ, United Kingdom*
[c] *Royal Netherlands Institute for Sea Research (NIOZ), Postbus 59, 1790 AB Den Burg - Texel, The Netherlands*
[d] *School of Earth, Ocean and Environmental Science (SEOES), University of Plymouth, Drake Circus, Plymouth PL4 8AA, United Kingdom*
[e] *National Oceanography Centre Southampton, University of Southampton, School of Ocean and Earth Science, European Way, Southampton SO14 3ZH, United Kingdom*
[f] *LOB, Parc Scientifique et Technologique de Luminy, Case 901, F-13288 Marseille Cedex 09, France*

Received 24 April 2006; received in revised form 9 November 2006; accepted 15 November 2006
Available online 9 January 2007

Abstract

Aerosol (soluble and total) iron and water-column dissolved (DFe, <0.2 μm) and total dissolvable (TDFe, unfiltered) iron concentrations were determined in the Canary Basin and along a transect towards the Strait of Gibraltar, in order to sample across the Saharan dust plume. Cumulative dust deposition fluxes estimated from direct aerosol sampling during our one-month cruise are representative of the estimated deposition fluxes based on near surface water dissolved aluminium concentrations measured on board. Iron inventories in near surface waters combined with flux estimates confirmed the relatively short residence time of DFe in waters influenced by the Saharan dust plume (6–14 months). Enhanced near surface water concentrations of DFe (5.90–6.99 nM) were observed at the Strait of Gibraltar mainly due to inputs from metal-rich rivers. In the Canary Basin and the transect towards Gibraltar, DFe concentrations (0.07–0.76 nM) were typical of concentrations observed in the surface North Atlantic Waters, with the highest concentrations associated with higher atmospheric inputs in the Canary Basin. Depth profiles showed that DFe and TDFe were influenced by atmospheric inputs in this area with an accumulation of aeolian Fe in the surface waters. The sub-surface minimum of both DFe and TDFe suggests that a simple partitioning between dissolved and particulate Fe is not obvious there and that export may occur for both phases. At depths of around 1000–1300 m, both regeneration and Meddies may explain the observed maximum. Our data suggest that, in deep waters, higher particle concentrations likely due to dust storms may increase the scavenging flux and thus decrease DFe concentrations in deep waters.

Keywords: Dissolved iron; Total dissolvable iron; Aerosol deposition; Solubility; Scavenging; Regional terms: North-East Atlantic; Canary Basin; Madeira; Gibraltar

* Corresponding author. Tel.: +33 2 98 49 86 55; fax: +33 2 98 49 86 45.
E-mail address: Geraldine.Sarthou@univ-brest.fr (G. Sarthou).
[1] Present address: DOP-DCB-TSI-ME, IFREMER, BP 70, F-29280 Plouzané, France.

0304-4203/$ - see front matter © 2006 Elsevier B.V. All rights reserved.
doi:10.1016/j.marchem.2006.11.004

1. Introduction

Iron (Fe) is a key nutrient for all organisms. It is used in a variety of enzyme systems, including those for photosynthesis, respiration, and nitrogen fixation (Falkowski et al., 1998; Morel and Price, 2003). Over the past 15 years, Fe has become recognized as a prime limiting element for phytoplankton in several large parts of the global ocean (Martin et al., 1994; Coale et al., 2004). Fe availability not only controls the primary productivity, but can also regulate the structure and the composition of planktonic communities (Coale et al., 1996, 2004; de Baar and Boyd, 2000; Hutchins et al., 2002). The limiting concentrations of Fe are mainly due to the very low solubility of Fe(III), which is the thermodynamically favoured redox state of iron in oxic waters (Liu and Millero, 2002). Fe(III) in seawater rapidly forms colloidal and particulate phases and/or is scavenged by these phases (Byrne and Kester, 1976; Wu and Luther, 1994; Johnson et al., 1997). More than 99% of the dissolved Fe in seawater is complexed by dissolved organic ligands (Gledhill and van den Berg, 1994; van den Berg, 1995; Wu and Luther, 1995; Rue and Bruland, 1995, 1997). These ligands increase Fe solubility in seawater and the organic fraction of iron appears to be an important pool for phytoplankton cells, either directly by dissociation of the organic complex or via (photo-) reduction (Hutchins et al., 1999; Kuma et al., 2000; Wells and Trick, 2004; Rose et al., 2005). The abundance and bioavailability of Fe is controlled by a combination of processes including various sources, sinks and internal cycling that are still largely unknown.

Table 1
Trace metal aerosol sample collection details and dry deposition fluxes of soluble Fe ($SolFe_a$), soluble Al ($SolAl_a$), total Fe (TFe_a) and total Al (TAl_a) in nmol m^{-2} d^{-1}

Sample number[a]	Start date and time (UTC)	Start position	End date and time (UTC)	End position	Sampling duration (h)	Air volume (m^3)	$SolFe_a$	TFe_a	$SolAl_a$	TAl_a	$SolAl_a$/ $SolFe_a$	TAl_a/ TFe_a
P03	05/10/2002 09:30	35.1°N 23.8°W	06/10/2002 08:55	32.0°N 21.5°W	23.3	1580	192±4	4,680± 190	1,220± 100	22,100± 1000	6.3	4.7
P04	06/10/2002 09:15	32.0°N 21.5°W	07/10/2002 08:55	30.0°N 20.0°W	22.0	1480	673±5	43,900± 400	6,720± 270	211,000± 1,600	10.0	4.8
P05	07/10/2002 09:15	30.0°N 20.0°W	08/10/2002 09:20	31.7°N 20.0°W	23.6	1600	180±2	10,900± 370	1,700±59	51,400± 1,400	9.4	4.7
P06	08/10/2002 09:40	31.7°N 20.0°W	09/10/2002 09:40	31.7°N 22.0°W	7.4	502	22±4	169±25	118±6	1,190±43	5.4	7.0
P07	09/10/2002 10:00	31.7°N 22.0°W	10/10/2002 09:40	31.6°N 24.0°W	18.7	1278	11±1	274±10	80±2	929±17	7.4	3.4
P08	10/10/2002 10:00	31.6°N 24.0°W	13/10/2002 11:10	25.0°N 23.8°W	35.1	2380	15±1	286±6	70±1	744±11	5.6	2.6
P09	13/10/2002 11:30	25.0°N 23.8°W	14/10/2002 09:10	25.0°N 21.3°W	21.1	1431	14±2	70±40	77±8	450±14	5.7	6.4
P10	14/10/2002 09:30	25.0°N 21.3°W	15/10/2002 08:40	25.0°N 18.9°W	21.6	1464	12±3	178±8	61±3	551±14	5.2	3.1
P11	15/10/2002 09:00	25.0°N 18.9°W	20/10/2002 09:10	27.4°N 25.4°W	27.6	1871	10±2	104±7	53±4	554±12	5.1	5.3
P13	20/10/2002 09:30	27.4°N 25.4°W	22/10/2002 09:40	25.7°N 19.0°W	47.0	3187	7±3	41±4	41±2	207±7	5.3	5.1
P14	22/10/2002 10:00	25.7°N 19.0°W	24/10/2002 09:40	30.0°N 17.5°W	44.8	3037	9±1	99±4	31±1	406±8	3.5	4.1
P15	24/10/2002 10:00	30.0°N 17.5°W	25/10/2002 09:00	32.1°N 17.0°W	22.8	1546	<0.7	<19	12±5	48±15	n.d.	n.d.
F^{av}							82±1	4,310±42	724±21	20,500± 170		
D^{cum}							1.22±0.01	61.9±0.6	10.6±0.3	294.0±2.6		

Also reported are Al/Fe ratios for soluble and total fractions. Standard deviations represent the influence of propagated analytical errors on calculated deposition fluxes, but do not include the 2–3 fold uncertainty in deposition velocity. The average deposition fluxes (F^{av}) and the cumulative deposition over the 20 days of sampling (D^{cum}, μmol m^{-2} $(20\ d)^{-1}$) were calculated using Eqs. (2) and (3) (see text). Dates are in DD/MM/YYYY format.

n.d. not determined.

[a] Samples P01 and P02 were an operational blank (filter mounted in cassette, but not deployed in collector) and an exposure blank (filter deployed in collector, but not switched on) respectively.

Aeolian dust transport, mainly from the great deserts of the world, represents the dominant external input of iron to the surface of the open ocean (Jickells et al., 2005). The arid areas are very sensitive to global change (Prospero et al., 2002; Gong et al., 2004), hence they could have a strong impact on ocean primary productivity and climate. A better knowledge and understanding of Fe distributions, sources and sinks in the oceanic regions influenced by these areas is then crucial for an accurate interpretation of Fe biogeochemistry and its impact on global climate change. The North Atlantic Ocean receives nearly half (43%) of the total dust input to the global ocean (Jickells et al., 2005), primarily due to the proximity of the Sahara desert (Prospero, 1996). Dust production, transport and deposition processes are highly variable. Over the Atlantic Ocean, half of the annual deposition occurs in about 10 weeks (Swap et al., 1996), and in the Canary Basin, episodic dust pulses last an average of 3–8 days, occurring mainly in winter and summer/fall (Pérez-Marrero et al., 2002; Torres-Padron et al., 2002).

Here we report water-column (dissolved and total dissolvable) and aerosol Fe concentrations in a high atmospheric input region, the Canary Basin. Regions with lower and/or contrasting Fe inputs such as the area between Madeira and Gibraltar or the Strait of Gibraltar itself were also investigated. These data are used to interpret and quantify the impact of atmospheric Fe inputs on Fe distribution, residence time and scavenging processes.

2. Sampling and methods

Aerosol and seawater samples were collected aboard the R.V. Pelagia between October 7 and October 29, 2002, during the IRONAGES III shipboard expedition-between Ponta Delgada (Azores, Portugal) and Valencia (Spain).

2.1. Aerosol samples

Aerosol samples for Fe and Al analyses were collected with a high volume (1 m^3 min^{-1}) sampler (Graseby–Anderson) on acid-washed cellulose filters (Whatman 41). Details of sample collection are given in Table 1. Soluble metals were extracted using an ammonium acetate leach at pH 4.7 for 1–2 h (Sarthou et al., 2003). This pH was chosen initially as a mimic for release of trace metals from aerosol in rainwater, but is similar to a procedure employed by Bruland et al. (1991) to examine the bioavailable Fe content of upwelled particulate matter off the coast of California. Baker et al. (2006) concluded that the pH 4.7 leach may over-estimate Fe solubility by a varying amount, depending on the strength of organic complexation of Fe in the receiving waters. Portions of each filter were cut into small pieces with acid-washed, ceramic-bladed scissors and suspended in 25 mL of buffer solution for 1–2 h, after which the supernatant was filtered (0.2 μm, cellulose acetate filter, minisart, Sartorius) and acidified with 69% Aristar HNO_3 to 0.4% v/v HNO_3. A strong acid digestion procedure was used to determine total Fe and Al. Aerosol filter portions were boiled to dryness firstly in 69% Aristar HNO_3 and then in 40% HF (Aristar, BDH) to destroy organic matter (including the cellulose filter) and the aluminosilicate matrix of the mineral component of the aerosol (Baker et al., 2006). The residue was redissolved in 1 M HNO_3, transferred quantitatively to 25 mL volumetric flasks and made up to volume. Fe and Al concentrations in the extracts were determined by inductively coupled plasma-optical emission spectroscopy (ICP-OES, Varian, Vista-Pro). Filter blanks were determined with unexposed, acid-washed filters. Procedural blanks, in which filter papers were loaded into sampling cassettes for ~24 h but with no air drawn through them, showed no significant increase in concentration. Concentrations in extracts (C) were converted into atmospheric concentrations by calculating the total quantity (Q) of Fe and Al on each filter, after appropriate blank correction, and dividing by the known volume of air (V) filtered for each sample. Uncertainties quoted for atmospheric concentrations have been calculated from standard deviations of replicate analyses and propagated for each stage of data analysis (blank subtraction etc.) by standard error propagation methods. Deposition fluxes for each sample (F) were calculated from atmospheric concentrations using a deposition velocity (v_d) of 0.01 m s^{-1} (Eq. (1); Duce et al., 1991) and average deposition fluxes (F^{av}) were calculated using total quantities and sample volumes over the whole cruise (Eq. (2)).

$$F_x = (Q_x/V_x)v_d = C_x v_d \tag{1}$$

$$F_x^{av} = \frac{\sum Q_x}{\sum V_x} v_d \tag{2}$$

Cumulative deposition (D^{cum}) over the course of the cruise was calculated from Eq. (3), where t is the collection time for each sample.

$$D^{cum} = \sum F_x t_x \tag{3}$$

In making this calculation we assume that the deposition flux determined for each sample is representative of the whole study region.

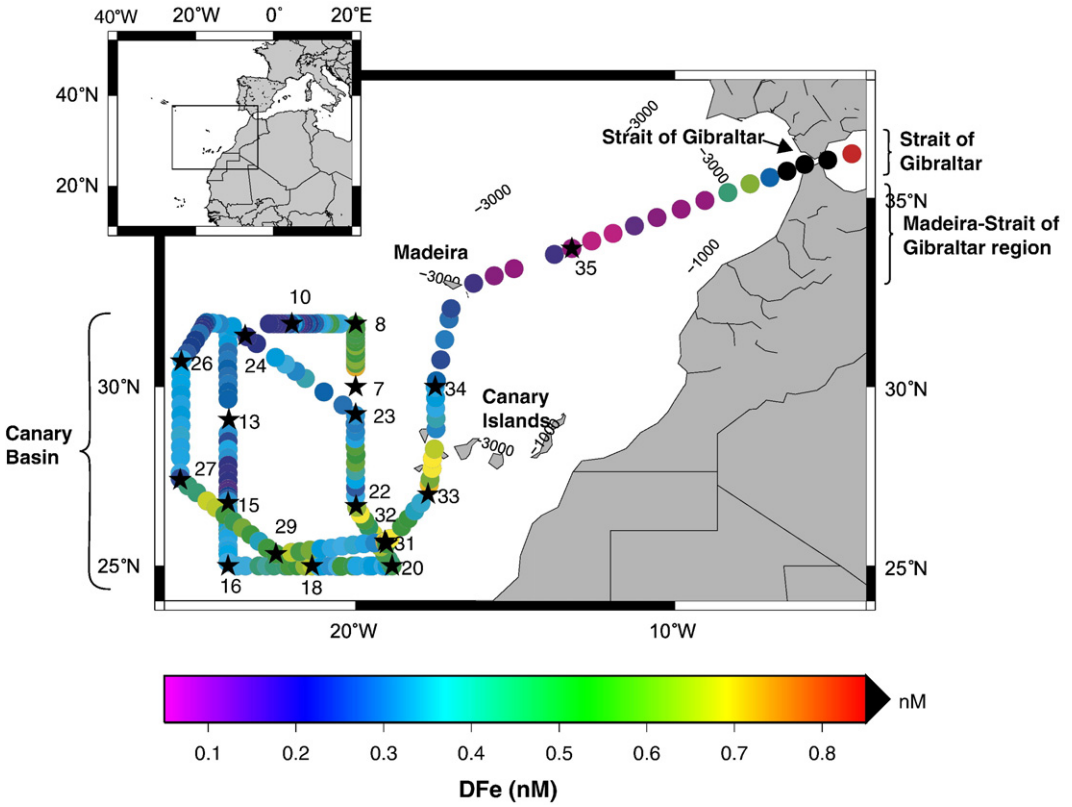

Fig. 1. Contour map showing near surface water dissolved iron concentrations during the IRONAGES III cruise from October 7–29 aboard R.V. Pelagia. Points in black are values ranging from 5.9 to 7.0 nM. Stations are labelled as stars in the graph. A smaller scale of the research area is given in the inset map.

2.2. Seawater samples

The cruise track and positions of the sampling stations for seawater samples are shown in Fig. 1 and additional station details are reported in Table 2. Shallow surface water depth profiles (0–150 m) as well as deep profiles (0–4000 m) were collected. Samples for dissolved Fe (DFe, filtered,<0.2 μm) and total dissolvable Fe (TDFe, unfiltered) concentrations were obtained using Teflon coated PVC General Oceanics 12-L GoFlo bottles on an ultraclean CTD rosette sampler attached to an all-Kevlar cable with internal communication cables. At one of the deep casts (St 34-3), Go-Flo bottles were mounted on a 6 mm Kevlar hydrowire for comparison with the ultraclean CTD Rosette sampling system. Moreover, at station 34 (34-1, 34-2 and 34-3), an on board intercalibration of DFe methods was carried out with a similar FIA technique (de Jong et al., 1998). Filtered samples for DFe analysis were collected from Go-Flo bottles using slight N_2 overpressure and filtration through 0.2 μm filter cartridges (Sartrobran-300, Sartorius). Underway near surface water sampling was conducted during transit between the stations. Samples were collected every 1–2 h with a fish towed from a winch extended ca. 5 m from the ship's starboard side and deployed at 1–2 m below the surface (Sarthou et al., 2003; Kramer et al., 2004). Surface water was pumped on-board with an all Teflon Bellows pump directly into a clean-container and filtered on-line through a 0.2 μm filtration cartridge (Sartobran-P, Sartorius). For DFe analysis, filtered samples were acidified to pH 2.0 with 1 mL of ultrapur® hydrochloric acid (HCl, Merck) per 1 L of sample for at least 24 h before analysis on board. During the SAFE cruise, an acidification at pH 2.0 for at least 24 h allowed us to recover more than 98% of total dissolved Fe, whereas only 62% was recovered after 10 h of acidification. For TDFe, unfiltered samples were also acidified at pH 2.0 and stored at least 6 months before measurement in the laboratory in order to release all but the most refractory Fe species into the dissolved form (Löscher et al., 1997).

DFe and TDFe concentrations were measured using a chemiluminescence method adapted from Obata et al.

Table 2
DFe and TDFe concentrations for shallow (0–150 m) and deep (0–4000 m) vertical profiles

Station-cast	Depth (m)	DFe (nM)	STD DFe (nM)	TDFe (nM)	STD TDFe (nM)	LPFe (nM)
7-4	10	0.54	0.03	2.95	0.00	2.42
07/10/2002	25	0.47	0.03	n.d.	–	–
30.00°N 20.00°W	50	0.38	0.01	0.54	0.01	0.16
	60	0.34	0.00	0.70	0.02	0.36
	80	0.37	0.01	0.48	0.01	0.11
	100	0.44	0.03	1.40	0.11	0.96
	125	0.36	0.01	0.66	0.01	0.29
	150	0.46	0.02	1.50	0.06	1.03
8-1	10	0.50	0.04	n.d.	–	–
08/10/2002	25	0.57	0.02	n.d.	–	–
31.71°N 20.00°W	60	0.36	0.01	n.d.	–	–
	80	0.23	0.00	n.d.	–	–
	100	0.26	0.01	n.d.	–	–
	125	0.35	0.03	n.d.	–	–
	150	0.56	0.02	n.d.	–	–
10-1	10	0.19	0.00	0.78	0.00	0.59
09/10/2002	25	0.18	0.00	0.71	0.00	0.53
31.71°N 22.00°W	50	0.11	0.01	0.43	0.02	0.32
	60	0.10	0.00	0.33	0.01	0.23
	70	0.13	0.01	0.21	0.02	0.08
	80	0.10	0.02	0.19	0.00	0.09
	90	0.08	0.00	0.23	0.00	0.15
	100	0.13	0.01	0.27	0.01	0.15
	125	0.23	0.01	n.d.	–	–
10-2	200	0.19	0.01	n.d.	–	–
09/10/2002	400	0.46	0.03	n.d.	–	–
31.71°N 22.00°W	600	0.46	0.01	1.19	0.03	0.73
	1300	0.64	0.04	1.12	0.02	0.48
	1600	0.52	0.03	1.00	0.02	0.48
	2000	0.51	0.04	0.96	0.01	0.45
	4000	0.59	0.01	0.81	0.01	0.23
13-1	10	0.41	0.01	n.d.	–	–
11/10/2002	25	0.44	0.01	n.d.	–	–
29.62°N 23.98°W	50	0.48	0.03	n.d.	–	–
	90	0.25	0.02	n.d.	–	–
	100	0.41	0.01	n.d.	–	–
	125	0.40	0.01	n.d.	–	–
	150	0.51	0.01	n.d.	–	–
15-1	10	0.52	0.00	n.d.	–	–
12/10/2002	25	0.55	0.00	n.d.	–	–
26.78°N 24.00°W	50	0.38	0.00	n.d.	–	–
	60	0.25	0.01	n.d.	–	–
	70	0.26	0.00	n.d.	–	–
	80	0.25	0.01	n.d.	–	–
	90	0.29	0.01	n.d.	–	–
	100	n.d.	–	n.d.	–	–
	125	0.26	0.01	n.d.	–	–
	150	0.26	0.01	n.d.	–	–
16-1	10	0.37	0.01	n.d.	–	–
13/10/2002	50	0.22	0.01	n.d.	–	–
25.00°N 24.00°W	60	0.22	0.01	n.d.	–	–
	80	0.12	0.01	n.d.	–	–
	90	0.25	0.01	n.d.	–	–
	100	0.18	0.02	n.d.	–	–
16-1	125	0.33	0.01	n.d.	–	–
13/10/2002	150	0.43	0.00	n.d.	–	–
25.00°N 24.00°W						
18-1	10	0.63	0.02	n.d.	–	–
14/10/2002	25	0.67	0.00	3.86	0.06	3.18
25.00°N 21.37°W	60	0.31	0.03	2.39	0.16	2.08
	80	0.14	0.00	1.42	0.01	1.28
	90	0.13	0.00	0.83	0.02	0.70
	100	0.19	0.00	1.03	0.11	0.84
	125	0.23	0.01	n.d.	–	–
	150	0.43	0.01	2.96	0.05	2.54
20-1	10	0.35	0.05	1.23	0.03	0.87
15/10/2002	25	0.28	0.00	1.32	0.01	1.04
25.00°N 18.86°W	50	0.24	0.00	0.56	0.05	0.31
	60	0.21	0.01	0.52	0.00	0.30
	70	0.29	0.01	0.67	0.01	0.38
	80	0.32	0.02	0.80	0.02	0.47
	90	0.36	0.02	1.02	0.05	0.66
	100	0.46	0.03	2.17	0.09	1.71
	125	0.70	0.04	2.15	0.00	1.45
	150	0.75	0.05	5.52	0.00	4.76
22-1	10	0.29	0.00	n.d.	–	–
16/10/2002	25	0.37	0.01	n.d.	–	–
26.70°N 19.99°W	50	0.21	0.01	n.d.	–	–
	60	0.28	0.01	n.d.	–	–
	90	0.23	0.01	n.d.	–	–
	100	0.25	0.00	n.d.	–	–
	150	0.41	0.00	n.d.	–	–
23-1	10	0.19	0.00	n.d.	–	–
17/10/2002	25	0.22	0.01	n.d.	–	–
29.25°N 20.03°W	50	0.21	0.01	n.d.	–	–
	60	0.22	0.01	n.d.	–	–
	80	0.17	0.01	n.d.	–	–
	90	0.09	0.01	n.d.	–	–
	100	0.13	0.01	n.d.	–	–
	150	0.25	0.03	n.d.	–	–
24-1	10	0.28	0.00	n.d.	–	–
18/10/2002	25	0.18	0.02	n.d.	–	–
31.39°N 23.47°W	50	0.10	0.00	1.67	0.00	1.57
	60	0.09	0.00	1.42	0.10	1.33
	80	0.07	0.00	n.d.	–	–
	90	0.06	0.00	1.49	0.09	1.43
	100	0.08	0.00	1.25	0.02	1.16
	150	0.16	0.00	1.63	0.08	1.47
26-1	10	0.36	0.01	n.d.	–	–
19/10/2002	25	0.35	0.04	n.d.	–	–
30.70°N 25.47°W	70	0.18	0.01	n.d.	–	–
	80	0.20	0.00	n.d.	–	–
	90	0.22	0.01	n.d.	–	–
	100	0.18	0.01	n.d.	–	–
	150	0.27	0.01	n.d.	–	–
27-1	10	0.16	0.00	2.01	0.09	1.85
20/10/2002	25	0.17	0.01	0.98	0.02	0.82
27.43°N 25.50°W	50	0.20	0.01	1.00	0.06	0.80
	60	0.18	0.00	1.13	0.11	0.95
	70	0.16	0.01	1.43	0.10	1.27

Table 2 (*continued*)

Station-cast	Depth (m)	DFe (nM)	STD DFe (nM)	TDFe (nM)	STD TDFe (nM)	LPFe (nM)
27-1	80	0.16	0.01	0.60	0.03	0.44
20/10/2002	100	0.20	0.01	1.19	0.00	0.99
27.43°N 25.50°W	150	0.29	0.01	1.26	0.07	0.97
29-1	10	0.28	0.01	n.d.	–	–
21/10/2002	25	0.43	0.02	n.d.	–	–
25.33°N 22.50°W	50	0.23	0.01	n.d.	–	–
	60	0.17	0.00	n.d.	–	–
	70	0.12	0.01	n.d.	–	–
	80	0.17	0.00	n.d.	–	–
	90	0.19	0.01	n.d.	–	–
	100	0.22	0.01	n.d.	–	–
	150	0.29	0.01	n.d.	–	–
31-1	10	0.45	0.00	n.d.	–	–
22/10/2002	25	0.53	0.01	n.d.	–	–
25.70°N 19.87°W	60	0.43	0.01	n.d.	–	–
	70	0.42	0.02	n.d.	–	–
	80	0.39	0.02	n.d.	–	–
	90	0.39	0.00	n.d.	–	–
	100	0.35	0.00	n.d.	–	–
	150	0.43	0.02	n.d.	–	–
32-1	10	0.36	0.01	n.d.	–	–
22/10/2002	25	0.44	0.01	n.d.	–	–
25.64°N 19.39°W	60	0.39	0.02	n.d.	–	–
	70	0.42	0.01	n.d.	–	–
	80	0.42	0.00	n.d.	–	–
	90	0.42	0.00	n.d.	–	–
	100	0.33	0.01	n.d.	–	–
	125	0.30	0.01	n.d.	–	–
	150	0.36	0.01	n.d.	–	–
33-1	10	0.39	0.01	n.d.	–	–
23/10/2002	60	0.40	0.03	n.d.	–	–
27.27°N 17.73°W	70	0.26	0.02	n.d.	–	–
	80	0.28	0.01	n.d.	–	–
	90	0.19	0.00	n.d.	–	–
	100	0.35	0.01	n.d.	–	–
	125	0.25	0.01	n.d.	–	–
34-1	10	0.13	0.00	2.05	0.10	1.92
24/10/2002	25	0.14	0.01	1.50	0.02	1.36
30.00°N 17.50°W	50	0.21	0.01	n.d.	–	–
	60	0.15	0.00	0.51	0.01	0.36
	70	0.11	0.00	0.65	0.01	0.53
	80	0.10	0.00	0.79	0.02	0.69
	90	0.10	0.00	0.87	0.04	0.77
	100	0.12	0.00	0.77	0.03	0.65
	125	0.15	0.00	0.62	0.03	0.47
	150	0.24	0.01	1.07	0.06	0.83
34-2	100	0.19	0.01	n.d.	–	–
24/10/2002	735	0.36	0.01	n.d.	–	–
30.00°N 17.50°W	1000	0.52	0.01	n.d.	–	–
	1300	0.47	0.02	n.d.	–	–
	1600	0.44	0.01	2.14	0.05	1.70
	2000	0.37	0.02	n.d.	–	–
	3000	0.40	0.00	2.06	0.03	1.66
	4000	0.40	0.02	n.d.	–	–

Table 2 (*continued*)

Station-cast	Depth (m)	DFe (nM)	STD DFe (nM)	TDFe (nM)	STD TDFe (nM)	LPFe (nM)
34-3*	300	0.22	0.00	n.d.	–	–
24/10/2002	485	0.39	0.01	n.d.	–	–
30.00°N 17.50°W	700	0.43	0.00	n.d.	–	–
	750	0.42	0.01	n.d.	–	–
	1700	0.36	0.02	n.d.	–	–
	2700	0.37	0.01	n.d.	–	–
35-1	10	0.11	0.00	n.d.	–	–
27/10/2002	50	0.09	0.00	0.64	0.01	0.55
33.70°N 13.22°W	70	0.05	0.00	0.67	0.00	0.62
	80	0.05	0.00	n.d.	–	–
	90	0.10	0.00	0.49	0.04	0.40
	100	0.09	0.00	0.25	0.00	0.16
	125	0.10	0.00	0.89	0.00	0.79
	150	0.13	0.01	n.d.	–	–

LPFe = labile particulate Fe = TDFe − DFe. Standard deviation (STD) is calculated from triplicate analyses. STD values equal to 0.00 nM in the Table correspond to values lower than 0.005 nM. Dates are in DD/MM/YYYY format.

* At station 34–3, samples were collected with Go-Flo bottles hung on a 4000-m long Kevlar cable and not with the Go-Flo bottles mounted on an ultraclean CTD rosette sampling system attached to an all-Kevlar cable with internal communication cables, as for all the other stations.

(1993) (see Sarthou et al., 2003; Laës et al., 2003). The purification of the luminol solution through a column of 8-hydroxyquinoline (8-HQ) immobilised on hydrophilic vinyl polymer (TSK-8-HQ after Dierssen et al., 2001) improved both the blank and detection limit of the method. The blank was determined each day as the measurements of a low iron concentration sample with 0 s of preconcentration and varied between 0.001 and 0.083 nM with a mean value of 0.033 ± 0.023 nM (n = 40). The detection limit, equal to three times the standard deviation of the blank, ranged from 0.006 to 0.074 nM with an average value of 0.027 ± 0.017 nM (n = 40). The individual contributions to the total blank of ultrapur® hydrochloric acid (MERCK), suprapur® ammonia (MERCK), and ammonium acetate buffer purified three times through a 8-HQ column were determined by addition of increasing amounts of these reagents to the sample and were lower than our detection limit.

Dissolved aluminium (DAl) concentrations were measured concomitantly with DFe concentrations and the complete data set is published in Kramer et al. (2004). DAl is used as a tracer for the indication of dust input to the surface waters (Measures et al., 1984). It has a longer residence time than DFe and can be used to infer the cumulative aeolian input of DFe over seasonal to longer timescales (Measures et al., 2005).

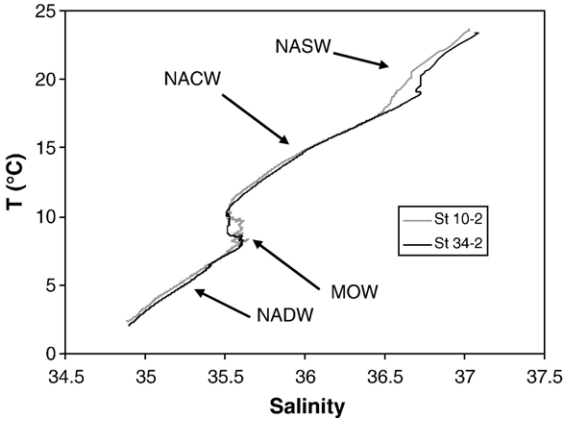

Fig. 2. Salinity vs. temperature for deep stations 10-2 and 34-2.

2.3. Ancillary measurements

2.3.1. Dissolved nutrients

Samples for dissolved nutrient analysis were collected in a high-density polyethylene sample bottle, filtered through 0.2 μm filter cartridges (Sartrobran-300, Sartorius) and stored in the dark at 4 °C in a polyethylene cup. All samples were analyzed within 8 h on a Technicon TrAAcs 800 autoanalyzer, except for some orthosilicic acid samples which were analysed within 24 h. The nutrients were measured colorimetrically as described by Grasshoff (1983).

2.3.2. Chlorophyll-a

Samples for Chlorophyll-*a* (Chl-*a*) (typically 1.5 L) were collected on a GF/F filter, after which they were stored at −80 °C. All samples were analysed during the cruise as described by Veldhuis and Kraay (2004).

3. Results

3.1. Study area

The general characteristics of the study area are detailed in Kramer et al. (2004). In most of the study area, low concentrations in the surface mixed layer (North Atlantic Surface Waters, NASW, Fig. 2, between 25 and 60 m, with an average value of 45 ± 10 m, $n = 19$) were observed for the major nutrients (0.2–0.5 μM Si $(OH)_4$, 0.01–0.04 μM PO_4^{3-}, <0.05 μM NO_3^-). A deep Chl-*a* maximum, typically between 50 and 150 m, was observed at each station with values between 0.13 and 0.54 μg/L.

The T–S diagram shows the different water masses for the two deep stations 10 and 34 (Fig. 2). Below the NASW, until approximately 700 m depth, the North Atlantic Central Water (NACW) is observed. At intermediate layers (1000–1300 m depth), the more saline Mediterranean Outflow Water (MOW) is present. More precisely, the MOW propagates large anticyclonic subsurface eddies, called Meddies, which help in maintaining the Mediterranean salt tongue in the North Atlantic (Richardson et al., 1989; Mazé et al., 1997; Hernandez-Guerra et al., 2005). Although their number in the Canary Basin is still uncertain (maybe around 25 at a time, Richardson, 1993), they are relatively common there and may exist as individual entities for as long as 2–3 years without completely mixing with Atlantic waters (Rossby, 1988). Below the MOW, we find the North Atlantic Deep Water (NADW), with salinity decreasing with depth.

The Canary Current, which flows along the African coast and entrains upwelled coastal water, might play a significant role in the east/southeast part of our study area, where a decrease in surface temperature and salinity and in the surface mixed layer depth indicates an influence of upwelled waters.

3.2. Total and soluble dry deposition fluxes

Total and soluble aerosol concentrations of Fe and Al are reported in Baker et al. (2006). Dry deposition rates were calculated from atmospheric concentrations using a deposition velocity of 0.01 m s^{-1}, appropriate for bulk (non-size segregated) aerosol (Duce et al., 1991). Uncertainties quoted for deposition fluxes have been calculated in the same way as for atmospheric concentrations, from standard deviations of replicate analyses and propagated for each stage of data analysis (blank subtraction, etc.) by standard error propagation methods. However, the deposition velocity estimation is a first approximation since velocities are poorly constrained and uncertainties may be as much as a factor 2–3 (Duce et al., 1991). Dry deposition rates for soluble and total Fe ($SolFe_a$ and TFe_a) and for soluble and total Al ($SolAl_a$ and TAl_a) are reported on Table 1. They vary between <0.7 and 673 nmol m^{-2} d^{-1} for $SolFe_a$, 12 and 6720 nmol m^{-2} d^{-1} for $SolAl_a$, <19 and 43,900 nmol m^{-2} d^{-1} for TFe_a, and between 48 and 211,000 nmol m^{-2} d^{-1} for TAl_a.

3.3. Near surface water DFe concentrations

A total of 206 underway near surface water samples, obtained using the towed fish, were analysed on board (see Fig. 1 and Supplementary Table). DFe results can be divided into three regions. The first region is located in the Strait of Gibraltar area with DFe values as high as 5.90–6.99 nM (mean value, 6.37 ± 0.56, $n = 3$). The

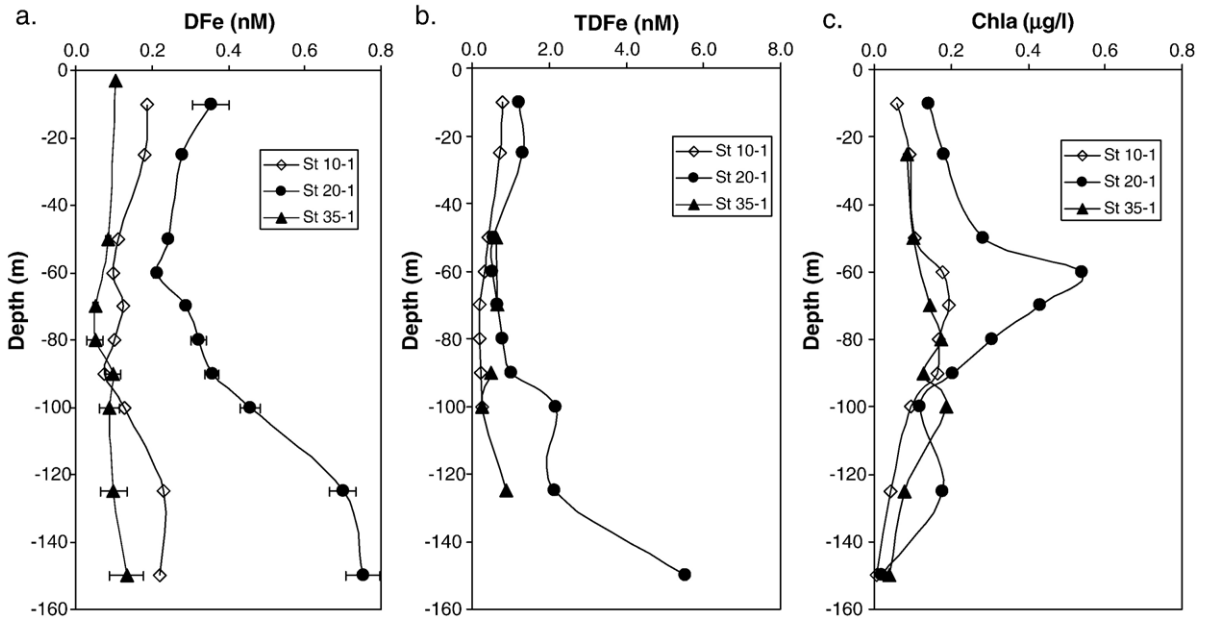

Fig. 3. Examples of vertical profiles of DFe (a), TDFe (b), and Chla-a (c) at station 10-1 (North-West part of the Canary Basin), station 20-1 (South-East part of the Canary Basin) and station 35-1 (transect towards Gibraltar). The error bars represent the standard deviation calculated from triplicate analyses.

second region is formed by the transect between Madeira and the Strait of Gibraltar, where the lowest values were observed, varying between 0.07 nM and 0.17 nM with an average value of 0.12±0.03 nM (n=11). The last region is the Canary basin, in a box from latitude 25°N to 32°N and longitude 17°W to 25°W, where concentrations ranged from 0.16 nM to 0.76 nM, with an average value of 0.39±0.14 nM (n=188). The highest concentrations in this zone were observed in the South/South-East part.

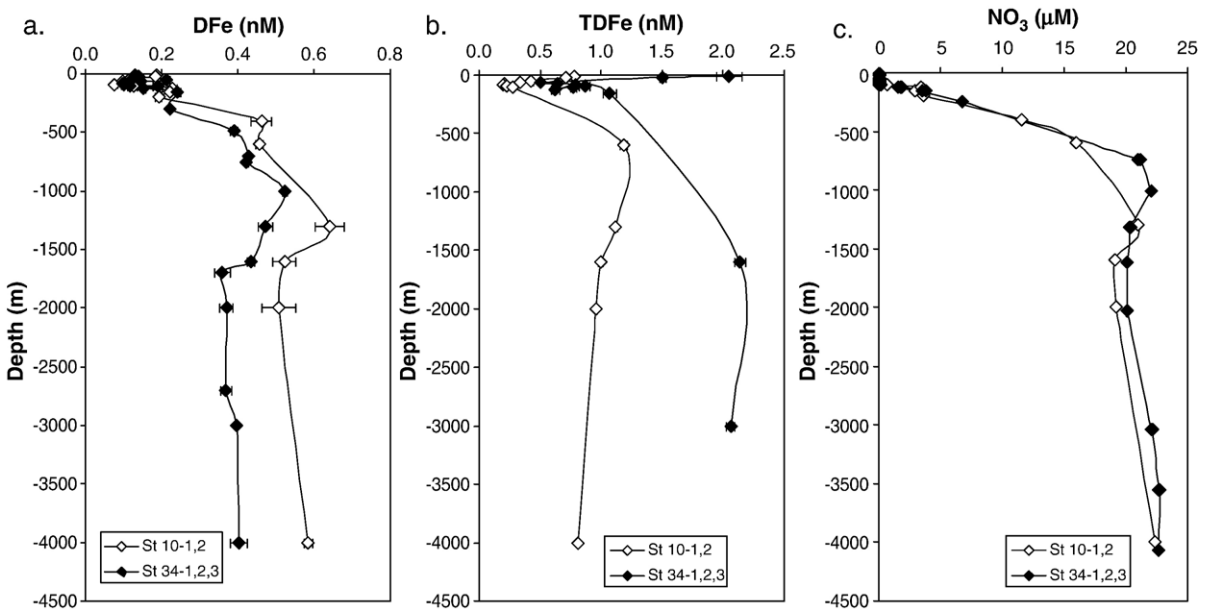

Fig. 4. Deep vertical profiles at station 10 and 34 of DFe (a), TDFe (b), and NO_3 (c). The error bars represent the standard deviation calculated from triplicate analyses.

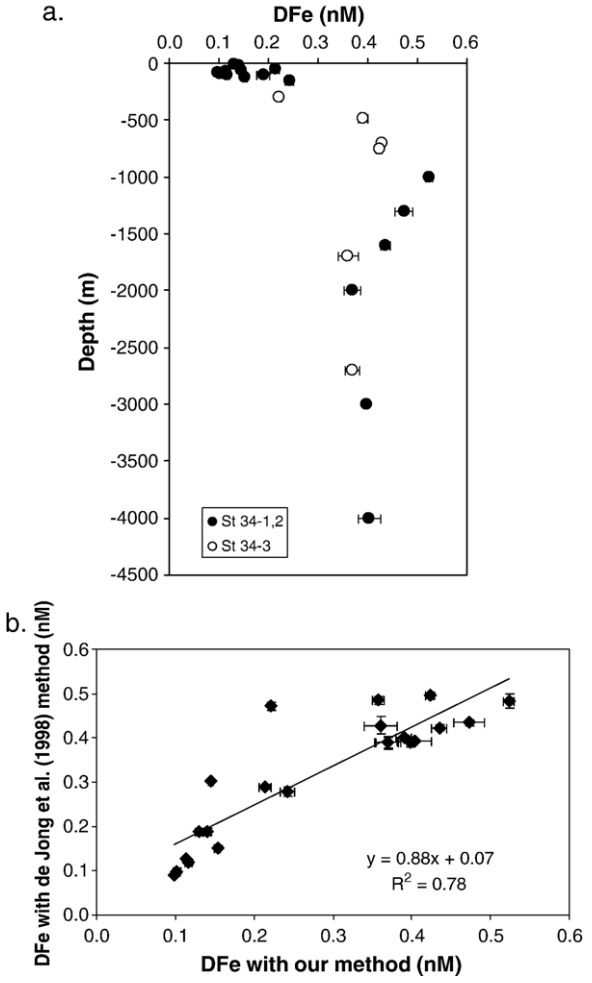

Fig. 5. (a) Depth profiles showing the DFe concentrations on samples collected using the clean CTD (filled circles) and GoFlo bottles mounted on a 6 mm Kevlar hydrowire (open circles). Same plot as Fig. 4a but with different symbols for the two sampling systems. (b) Results of the comparison between two analytical methods for the determination of DFe at station 34: DFe concentrations determined with our method vs. DFe concentrations determined with a similar FIA technique (de Jong et al., 1998).

3.4. Vertical profiles of DFe and TDFe

A total of 19 shallow vertical profiles (0–150 m) were analysed on board for DFe and 8 for TDFe back in the laboratory (see Table 2 and Fig. 1). Results are reported in Table 2 and three examples of typical DFe profiles are plotted on Fig. 3. DFe profiles show a maximum in the surface mixed layer, with values ranging for all stations from 0.09 nM to 0.67 nM, and a sub-surface minimum, with values between 0.05 nM and 0.35 nM. This sub-surface minimum corresponds with the deep chlorophyll maximum (DCM). Below the DCM, concentrations increase again to reach values between 0.13 nM and 0.75 nM. TDFe profiles show the same trend as DFe profiles with a surface maximum ranging from 0.64 nM to 3.86 nM, a sub-surface minimum (0.19 nM–1.25 nM), and values between 0.62 nM and 5.52 nM at 150 m.

Additionally, three deep casts were performed (stations 10 and 34, see Table 2 and Fig. 4). Below 150 m, DFe concentrations continue to increase until reaching a maximum around 1000 m of 0.64 nM and 0.52 nM for stations 10 and 34, respectively. Below 1500 m, at station 10, DFe varies between 0.51 nM and 0.59 nM with an average value of 0.54±0.04 nM (n=3). At station 34, values are slightly lower ranging from 0.36 nM to 0.43 nM with an average value of 0.39± 0.03 nM (n=6). At station 34, the ultraclean CTD Rosette sampling system (St 34-1 and 2) was successfully verified vs. individual Go-Flo samples mounted on a 6 mm Kevlar hydrowire (St 34-3, see Fig. 5a). Moreover, the intercalibration with another similar FIA technique (de Jong et al., 1998, see Fig. 5b) showed no significant difference between the two methods employed (Mann–Whitney test, p>0.1).

TDFe deep profiles (see Fig. 4b) show the same pattern as DFe deep profiles. TDFe concentrations at station 10 were 2 to 4 times lower than at station 34.

4. Discussion

4.1. Dry deposition fluxes

Dry deposition flux estimations vary between 2 to 3 orders of magnitude, with the highest values observed at the beginning of the cruise when dust was clearly visible on the filters. The mean aerosol TAl_a/TFe_a ratio of 4.7± 1.3 (n=11) is consistent with a primarily crustal origin of the material (Taylor and McLennan, 1985). The large range in dry deposition fluxes is due to the very high variability of dust production, transport and deposition processes. Our values of daily fluxes agree well with other soluble and total daily fluxes also estimated from aerosol samples collected on board in the North and Equatorial Atlantic (Sarthou et al., 2003; Croot et al., 2004b). As already mentioned by Croot et al. (2004b), daily flux estimates do not directly compare with modelled annual fluxes but do agree well with the overall pattern of dust deposition as predicted in other studies (Tegen and Fung, 1994; Mahowald et al., 1999, 2005).

Measures and Brown (1996) suggested that DAl concentrations of the surface layer might be used to

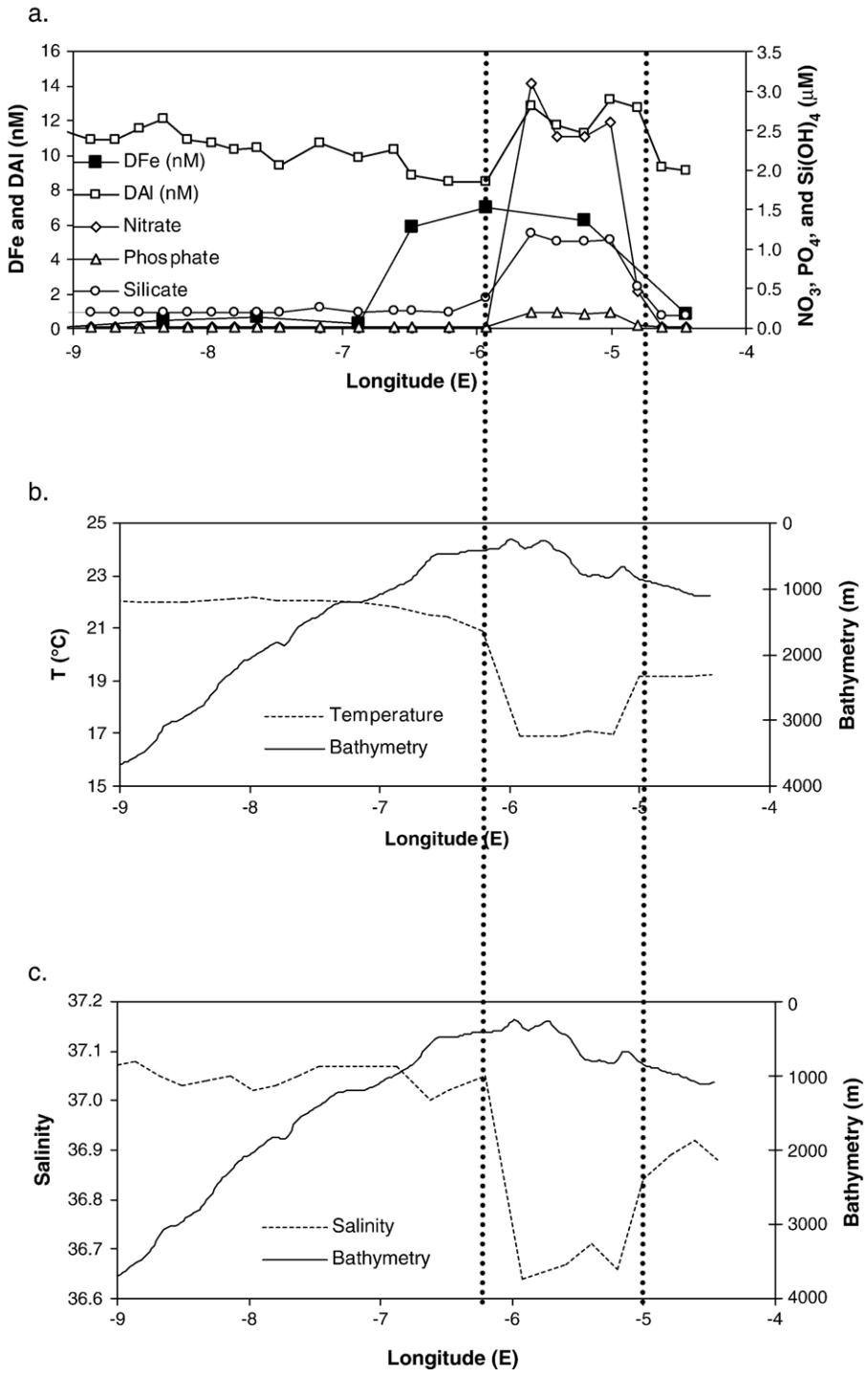

Fig. 6. (a) dissolved Fe, dissolved Al (from Kramer et al., 2004), nitrate, phosphate and silicate concentrations at sea-surface around the Strait of Gibraltar vs. longitude. (b) Sea-surface temperature and bathymetry around the Strait of Gibraltar vs. longitude. (c) Sea-surface salinity and bathymetry around the Strait of Gibraltar vs. longitude. Vertical dotted lines delimit the region of upwelled waters in the Strait of Gibraltar.

indirectly estimate dust deposition fluxes to surface ocean waters and they proposed a simple model to make those estimations. Their model assumes that all the DAl in surface waters of the open ocean derives from the partial dissolution of aeolian dust deposited into the surface mixed layer. It is further assumed that between

1.5% and 5% of the deposited dust dissolves in this surface-mixed layer and that the DAl thus supplied has a 5-year residence time. Kramer et al. (2004) used DAl data from our cruise together with this model to estimate average annual fluxes to the Canary Basin of 1.0–2.2 g dust m^{-2} y^{-1}, assuming a mixed layer depth of 50 m and an Al solubility of 3.25% (very similar to the value of 3.0% estimated for Saharan dust aerosols (Baker et al., 2006)). Over the whole sampling of the cruise (~20 d), that would represent a total dust flux of 55–120 mg m^{-2}. The cumulative dust fluxes estimated from direct aerosol sampling during our cruise considering the total cumulative flux of 62 μmol m^{-2} and 294 μmol m^{-2} for Fe and Al (Table 1), and assuming 4.3% and 8% of Fe and Al content in the Saharan dust, were equal to 81–99 mg m^{-2}, which is very close to the estimated value using the model developed by Measures and Brown (1996). This suggests that, during our study, cumulative dust deposition fluxes estimated from direct aerosol sampling over a one-month period are representative of the deposition fluxes estimated over a longer time-scale based on near surface water dissolved aluminium concentrations measured on board. Combining the deposition flux of soluble aerosol Fe and DFe inventory in the surface mixed layer, residence time for DFe with respect to dry deposition can be estimated in the Canary Basin (Sarthou et al., 2003; Croot et al., 2004b). DFe inventory was calculated as the average near-surface water concentrations in the Canary Basin (0.39 nM) multiplied by the average mixed layer (45 m). For the deposition flux of soluble Fe, we considered both the average deposition fluxes of soluble Fe measured on board (Eq. (2); Table 1) and the deposition fluxes of soluble Fe estimated using the model developed by Measures and Brown (1996), considering a value of Fe solubility for dust aerosols 1.7% (Baker et al., 2006). This estimation is a first approximation since the other fluxes (advection and diffusion) are not taken into account and we consider that the DFe concentrations and the atmospheric deposition we measured or estimated are representative in relation to the residence time of water column Fe. The estimated residence time for DFe relative to atmospheric inputs varied between 6 and 14 months, which is consistent with residence times of DFe in the surface waters of the North or Equatorial Atlantic (~10 days–1 year, Jickells, 1999; de Baar and de Jong, 2001; Sarthou et al., 2003; Croot et al., 2004b). Recent estimates in the central North Pacific or in the Red Sea also suggest a residence time of about half a year for DFe in surface waters of these regions (Boyle et al., 2005; Chase et al., 2006). These relatively short residence times of DFe allow the observation of inter-annual and intra-annual variations of DFe in the surface waters, as well as spatial heterogeneities, due to short variations of dust inputs or mesoscale activity (Boyle et al., 2005; Chase et al., 2006).

4.2. Underway near-surface water DFe

Near-surface water DFe concentrations observed around the Strait of Gibraltar were higher than previously reported for surface waters in this area (1–2 nM, Morley et al., 1997; Yoon et al., 1999), and enriched compared to the North Atlantic Surface Waters (Martin et al., 1993; de Jong et al., 2000; Boye et al., 2003; Laës et al., 2003; Blain et al., 2004). An increase was also observed for nitrate, phosphate, and silicate concomitant with a decrease in temperature and salinity at sea-surface (Fig. 6). This increase can be attributed to tide-induced mixing events at the sill of the Strait of Gibraltar between colder nutrient- and Fe-rich Mediterranean Outflowing Waters (MOW) and warmer nutrient- and Fe-poor Atlantic inflow Waters (AW, Gomez et al., 2000). An additional source of Fe to the surface waters may have come from shelf sediments during upwelling of waters at the sill because surface DFe concentrations at the Strait of Gibraltar were higher than deep DFe concentrations in the western basin of the Mediterranean Sea or in the NACW (Yoon et al., 1999; Sarthou and Jeandel, 2001; Guieu et al., 2002). Moreover, the DFe increase is observed west of where all the other elements start to increase and temperature and salinity to strongly decrease due to upwelling of deep waters. This suggests that another source of DFe exists west of the Strait of Gibraltar. These high enrichments in the Gulf of Cadiz, already observed for some other trace metals, were attributed to the Tinto and Odiel discharge occurring along the coast of the Gulf of Cadiz, which can provide up to 20% of the AW into the Strait of Gibraltar (van Geen et al., 1991; Elbaz-Poulichet et al., 2001a). Usually, high Fe concentrations in the rivers are rapidly removed due to scavenging processes in the estuaries. However, in the Odiel and Tinto mixing zone, Fe removal is relatively reduced compared to "typical" estuaries due to higher iron solubility in low pH waters (Elbaz-Poulichet et al., 1999). Very high Al concentrations were previously observed in the Odiel and Tinto mixing zones (Elbaz-Poulichet et al., 1999) but, during our study, relatively low Al concentrations were observed on the same samples as for our Fe concentrations (Kramer et al., 2004). Both Fe(III) and Al(III) hydroxide solubilities increase when pH decreases (Hall et al., 1980; Millero, 1998), but low pH also helps to

stabilise Fe(II), a much more soluble species of Fe, which could be further stabilised by complexation with some organic ligands (Santana-Casiano et al., 2000; Welch et al., 2002). Our results may also suggest that iron from the river plume is more efficiently remineralised and transported than aluminium. Finally, the sediments of this coastal sea have high metal levels (E.P.A., unpublished data). Al will most likely be less influenced by benthic reductive mobilisation processes then Fe. Hence the sediments will sustain higher DFe concentrations compared with DAl. East of the Strait, DFe values dropped from ~6 nM to less than 1 nM. This sharp decrease was also observed for the major nutrients in our study (from 2.61 to 0.02 μM for NO_3^-, from 0.21 to 0.02 μM for PO_4^{3-}, and from 1.12 to 0.16 μM for $Si(OH)_4$), as well as in a previous study (Gomez et al., 2000). In this latter study, in September, the clear decrease in nitrate concentrations east of the Strait was suggested to be related to the uptake by the very abundant phytoplankton community (Gomez et al., 2000), which could also explain the strong decrease in DFe and nutrient concentrations during our study.

Because the AW is the main water source of the Mediterranean Sea, enrichments in the Gulf of Cadiz may influence Fe concentrations in the whole Mediterranean basin. Indeed, a reassessment of DFe inflowing fluxes at the Strait of Gibraltar, using a recently estimated average transport for the AW ($25.6\ 10^{15}$ kg y^{-1}, Baschek et al., 2002; Gomez, 2003) would give a value of $164 \pm 15\ 10^6$ mol y^{-1}, which falls in the range of variations in estimated atmospheric and river inputs of the western Mediterranean Basin ($93–424\ 10^6$ mol y^{-1}, Guieu et al., 1997; Ridame et al., 1999; Elbaz-Poulichet et al., 2001b). However, DFe data at the Strait are still scarce and more data are needed to confirm our estimation.

In the Canary Basin near surface water DFe concentrations were higher than along the transect between Madeira and the Strait of Gibraltar (see Fig. 1), and not correlated with DAl concentrations (Kramer et al., 2004). DFe were higher in the south/south-east part, near the coastal upwelling area, indicating the influence of the proximity of the North West African continental margin. Near the North West African coast, upwelling is reported to occur throughout the year between 20 and 30°N, with peak intensity in July/August, and upwelling filaments have been reported that extend as far as 200 to 300 km offshore (Mittelstaedt, 1991). During our study, upwelling was only clearly detected in the south western part of the sampling grid and due to the southward movement of the Canary Current, this feature alone was unlikely to be the cause of the DFe gradient observed. However, it is hypothesised that the DFe gradient was a result of the continuous mixing of NACW with iron enriched shelf and coastal waters of the Iberian and North West African margin, transported offshore by upwelling and advection and entrained into the Canary Current.

The DFe and DAl data had opposing lateral gradients in the surface waters of the sampling grid (i.e. DAl concentrations were higher in the northwest part of the Canary Basin, Kramer et al., 2004). The difference between the distributions of both dissolved elements is further evidence that their residence times are significantly different in surface waters. A similar trend to the data reported here was observed in the North West Pacific Ocean by Johnson et al. (2003) for a transect from California to Hawaii. The waters influenced by continental margin sediments appear to be enriched in iron, relative to aluminium. This may result from diagenetic remobilization of iron in coastal sediments, which enriches surface sediment with iron (Johnson et al., 2003).

4.3. Vertical distributions of seawater DFe and TDFe

The vertical profiles confirm that DFe concentrations were highly influenced by atmospheric inputs in our study area. Indeed they all show a maximum of concentrations in near surface waters (0.09–0.67 nM), reflecting aeolian iron that accumulates in the oligotrophic surface mixed-layer (Bruland et al., 1994; Sarthou and Jeandel, 2001; Guieu et al., 2002; Wu and Boyle, 2002; Sedwick et al., 2005). These values are higher than the inorganic Fe(III) solubility (~0.1 nM, Wu et al., 2001) and could be explained by the strong organic complexation of iron (Boye et al., 2001, 2005; Croot et al., 2004a). Dissolved iron ligand concentrations as well as conditional stability constants were measured in the upper 150-m during the cruise and data are reported in detail elsewhere (Gerringa et al., 2006). Ligands concentrations were found to be in excess of DFe, with conditional stability constants ranging from $10^{19.5}$ to 10^{22} (Gerringa et al., 2006). In the surface mixed layer, high concentrations of organic ligands were attributed to a remnant of past blooms or present production under stressed conditions and/or a direct input from Sahara dust (Gerringa et al., 2006).

Below the surface mixed-layer, the sub-surface minimum of DFe (0.05–0.35 nM) corresponds to the DCM. This may have been due to removal *via* biological uptake and/or particle scavenging (Hutchins et al., 1993; Bruland et al., 1994). The subsurface minimum of DFe may also reflect the low Fe concentrations in the deeper mixed layer of the preceding spring period (Sarthou and Jeandel, 2001;

Sedwick et al., 2005). High concentrations of ligands concentrations were also determined in the DCM, probably from phytoplankton origin due to cell lysis (Gerringa et al., 2006). Despite the presence of these dissolved ligands, their affinity was not sufficient to maintain Fe in the dissolved phase. Our depth profiles of TDFe also showed a sub-surface minimum below the mixed layer, which could also reflect vertical mixing. In the Equatorial Pacific in Autumn and Sargasso Sea in summer both dissolved and particulate Fe were also removed around the DCM (Croot et al., 2004b; Sedwick et al., 2005). Sedwick et al. (2005) suggested that since a simple partitioning between dissolved and particulate Fe was not observed, vertical export of Fe might occur. Another similarity with our study area and the Sargasso Sea is the predominance of pico-plankton (*Prochlorococcus* for the Sargasso Sea, Sedwick et al., 2005, and *Synechococcus*, *Prochlorococcus*, and two groups of pico-eukaryotes for the Canary Basin, Gerringa et al., 2006). Our data also suggest that these groups of pico-plankton are adapted to low-light and low-iron and are able to exploit these conditions where the growth of other phytoplankton may be co-limited by light and iron (Sedwick et al., 2005; Veldhuis et al., 2005).

Below the DCM, DFe concentrations increase with depth to reach a maximum around 1000–1300 m (0.64 nM at station 10 and 0.52 nM at station 34). These values are consistent with the previously observed maxima around 1000 m in the North-East Atlantic (0.53–0.55 nM Martin et al., 1993; 0.62–0.86 nM, Laës et al., 2003). The maximum corresponds to both the maximum of nutrient regeneration and the occurrence of the Mediterranean Outflow Water (MOW, Fig. 2). Nitrate profiles reported on Fig. 4 show a maximum at depth 1000–1300 m due to remineralization of biogenic particles from the upper layers. This process is also a source of DFe in the water column and may then induce an increase in DFe concentrations. As estimated for DAl by Kramer et al. (2004), the observed DFe concentrations at station 10 and 34 (0.64±0.04 nM and 0.52±0.01 nM at 1000–1300 m with salinity of 35.64 and 35.62) are consistent with the simple dilution of a MOW end-member with a DFe concentration between 4.5±0.7 and 5.2±1.8 nM. These values are higher than previously observed in summer in the Gibraltar Outflow Water (1.09±0.40 nM, Morley et al., 1997), suggesting that both processes (remineralization and mixing with the MOW) may influence DFe concentrations around 1000 m.

Below 1000–1300 m, DFe concentrations slightly decrease to reach values of 0.40 and 0.59 nM at 4000 m for stations 34 and 10, respectively. These values are coherent with values observed in previous studies in the North Atlantic, although somewhat lower (0.74–0.82 nM, Laës et al., 2003; 0.64–0.76 nM, Martin et al., 1993). The difference can not be explained by an inter-method analytical difference because the same method has been used at least for our study and the study by Laës et al. (2003). The two main processes that constrain DFe concentrations in the deep waters are organic complexation and scavenging onto particles (Wu and Luther, 1994; Johnson et al., 1997). The concentrations of dissolved Fe-binding ligands were not determined in the deep water column during our study (Gerringa et al., 2006). However, concentrations of labile particulate Fe (LPFe, defined as the difference between TDFe and DFe, see Table 2) were five times higher at station 34 than at station 10, likely due to strong dust storm events (Ratmeyer et al., 1999). If the loss of DFe due to scavenging is function of both DFe and particle concentration, then a higher concentration of labile particulate Fe, associated with a higher particle concentration, will induce a higher scavenging sink of DFe (de Baar and de Jong, 2001; Parekh et al., 2005). The DFe/NO_3^- ratio is 1.5 times lower at station 34 than at station 10, confirming the hypothesis of higher scavenging at station at the former station. Parekh et al. (2005) showed that decreasing the scavenging ratio by 40% results in a ~0.1 nM increase in DFe in deep waters, which is the same order of magnitude as what is observed in our study.

5. Conclusion

The Canary Basin is a region with high atmospheric Fe inputs. Daily fluxes estimated from aerosol samples collected on board are in good agreement with other daily fluxes estimated in the North and Equatorial Atlantic as well as with longer timescale fluxes estimated from near surface water dissolved aluminium concentrations measured during our cruise. The opposite trend of dissolved Fe and Al in the near-surface waters of the Canary Basin reflects the difference in their residence times as well as the influence of the continental margin, which may be enriched in Fe relative to Al. A very contrasting feature in near surface DFe concentrations was observed at the Strait of Gibraltar with values one order of magnitude higher than in the other parts of our study, mainly due to inputs from metal-rich rivers.

Depth profiles of both DFe and TDFe reflect the impact of aerosol inputs on Fe cycle. Profiles show a maximum of concentrations in the surface waters and seem to be highly influenced by the amount of particulate

Fe in the deeper waters, which increases the sink of dissolved iron due to scavenging. In order to better quantify the variations of DFe in the deep waters, there is a need for further studies into the quantification of scavenging process with particle concentration and composition, as well as with organic ligands. Current models of the biogeochemical cycle of iron will only be improved when a better parameterisation of the scavenging process and of the role of ligands, as well as of the solubility and bioavailability of aeolian Fe will be available.

Acknowledgements

We wish to thank the officers and crew of the R.V. Pelagia for their professional and enthusiastic support during the cruise. The authors acknowledge M. Bossink for Chl *a* data and J.C. van Ooijen for nutrient data. This work was funded by the support from the European Commission's Marine Science and Technology Programme under Contract EVK2-1999-00227 (IRONAGES, ''Iron Resources and Oceanic Nutrients-Advancements of Global Environment Simulations''). E. Bucciarelli, two anonymous reviewers and W.M. Landing are gratefully acknowledged for their critical comments and suggestions. Contribution N° 1017 of the IUEM, European Institute for Marine Studies (Brest, France).

Appendix A. Supplementary data

Supplementary data associated with this article can be found, in the online version, at doi:10.1016/j.marchem.2006.11.004.

References

Baker, A.R., Jickells, T.D., Witt, M., Linge, K.L., 2006. Trends in the solubility of iron, aluminium, manganese and phosphorus in aerosol collected over the Atlantic Ocean. Mar. Chem. 98, 43–58.

Baschek, B., Send, U., Garcia-Lafuente, J.G., Candela, J., 2002. Transport estimates in the Strait of Gibraltar with a tidal inverse model. J. Geophys. Res. 106, 31033–31044.

Blain, S., Guieu, C., Claustre, H., Leblanc, K., Moutin, T., Quéguiner, B., Sarthou, G., 2004. Availability of iron and major nutrients for phytoplankton in the north-east Atlantic Ocean. Limnol. Oceanogr. 49 (6), 2095–2104.

Boye, M., van den Berg, C.M.G., de Jong, J.T.M., Leach, H., Croot, P., de Baar, H.J.W., 2001. Organic speciation of iron in the Southern Ocean. Deep-Sea Res., Part 1, Oceanogr. Res. Pap. 48, 1477–1497.

Boye, M., Aldrich, A., van den Berg, C.M.G., de Jong, J.T.M., Veldhuis, M., de Baar, H.J.W., 2003. Horizontal gradient of the chemical speciation of iron in surface waters of the northeast Atlantic Ocean. Mar. Chem. 80, 129–143.

Boye, M., Nishioka, J., Croot, P.L., Laan, P., Timmermans, K.R., de Baar, H.J.W., 2005. Major deviations of iron complexation during 22 days of a mesoscale iron enrichment in the open Southern Ocean. Mar. Chem. 96, 257–271.

Boyle, E.A., Bergquist, B.A., Kayser, R.A., Mahowald, N., 2005. Iron, manganese, and lead at Hawaii Ocean Time-series station ALOHA: temporal variability and an intermediate water hydrothermal plume. Geochim. Cosmochim. Acta 69 (4), 933–952.

Bruland, K.W., Donat, J.R., Hutchins, D.A., 1991. Interactive influence of bioactive trace metals on biological production in oceanic waters. Limnol. Oceanogr. 36 (8), 1555–1577.

Bruland, K.W., Orians, K.J., Cowen, J.P., 1994. Reactive trace metals in the stratified central North Pacific. Geochim. Cosmochim. Acta 58, 3171–3182.

Byrne, R.H., Kester, D.R., 1976. Solubility of hydrous ferric oxide and iron speciation in seawater. Mar. Chem. 4, 255–274.

Chase, Z., Paytan, A., Johnson, K.S., Street, J., Chen, Y., 2006. Input and cycling of iron in the Gulf of Aqaba, Red Sea. Glob. Biogeochem. Cycles 20 (3), GB3017. doi:10.1029/2005GB002646.

Coale, K.H., Fitzwater, S.E., Gordon, R.M., Johnson, K.S., Barber, R.T., 1996. Control of community growth and export production by upwelled iron in the equatorial Pacific Ocean. Nature 379, 621–624.

Coale, K.H., Johnson, K.S., Chavez, F.P., Buesseler, K.O., Barber, R.T., Brzezinski, M.A., Cochlan, W.P., Millero, F.J., Falkowski, P.G., Bauer, J.E., Wanninkhof, R.H., Kudela, R.M., Altabet, M.A., Hales, B.E., Takahashi, T., Landry, M.R., Bidigare, R.R., Wang, X.J., Chase, Z., Strutton, P.G., Friederich, G.E., Gorbunov, M.Y., Lance, V.P., Hilting, A.K., Hiscock, M.R., Demarest, M., Hiscock, W.T., Sullivan, K.F., Tanner, S.J., Gordon, R.M., Hunter, C.N., Elrod, V.A., Fitzwater, S.E., Jones, J.L., Tozzi, S., Koblizek, M., Roberts, A.E., Herndon, J., Brewster, J., Ladizinsky, N., Smith, G., Cooper, D., Timothy, D., Brown, S.L., Selph, K.E., Sheridan, C.C., Twining, B.S., Johnson, Z.I., 2004. Southern ocean iron enrichment experiment: carbon cycling in high- and low-Si waters. Science 304 (5669), 408–414.

Croot, P.L., Andersson, K., Ozturk, M., Turner, D.R., 2004a. The distribution and speciation of iron along 6°E in the Southern Ocean. Deep-Sea Res., Part 1, Oceanogr. Res. Pap. 51 (22–24), 2857–2879.

Croot, P.L., Streu, P., Baker, A.R., 2004b. Short residence time for iron in surface seawater impacted by atmospheric dry deposition from Saharan dust events. Geophys. Res. Lett. 31 (L23S08). doi:10.1029/2004GL020153.

de Baar, H.J.W., Boyd, P.M., 2000. The role of iron in plankton ecology and carbon dioxide transfert of the global ocean. In: Hanson, R.B., Ducklow, H.W., Field, J.G. (Eds.), The Changing Ocean Carbon Cycle: A Midterm synthesis of the Joint Global Ocean Flux Study. Cambridge University Press, Cambridge, pp. 61–140.

de Baar, H.J.W., de Jong, J.T.M., 2001. Distributions, sources and sinks of iron in seawater. In: Turner, D.R., Hunter, K.A. (Eds.), Biogeochemistry of Fe in Seawater. SCOR-IUPAC Series. J. Wiley, Baltimore, pp. 123–253.

de Jong, J.T.M., Den Das, J., Bathmann, U., Stoll, M.H.C., Kattner, G., Nolting, R.F., de Baar, H.J.W., 1998. Dissolved iron at subnanomolar levels in the Southern Ocean as determined by ship-board analysis. Anal. Chim. Acta 377 (2–3), 113–124.

de Jong, J.T.M., Boye, M., Schoemann, V.F., Nolting, R.F., de Baar, H.J.W., 2000. Shipboard techniques based on flow injection analysis for measuring dissolved Fe, Mn, and Al in seawater. J. Environ. Monit. 2, 496–502.

Dierssen, H., Balzer, W., Landing, W.M., 2001. Simplified synthesis of an 8-hydroxyquinoline chelating resin and a study of trace metal profiles from Jellyfish Lake, Palau. Mar. Chem. 73 (3–4), 173–192.

Duce, R.A., Liss, P.S., Merrill, J.T., Atlas, E.L., Buat-Ménard, P., Hicks, B.B., Miller, J.M., Prospero, J.M., Arimoto, R., Church, T.M., Ellis,

W., Galloway, J.N., Hansen, L., Jickels, T.D., Knap, A.H., Reinhardt, K.H., Schneider, B., Soudine, A., Tokos, J.J., Tsunogai, S., Wollast, R., Zhou, M., 1991. The atmospheric input of trace species to the world ocean. Glob. Biogeochem. Cycles 5 (3), 193–259.

Elbaz-Poulichet, F., Morley, N.H., Cruzado, A., Velasquez, Z., Achterberg, E.P., Braungardt, C.B., 1999. Trace metal and nutrient distribution in an extremely low pH (2.5) river-estuarine system, the Ria of Huelva (South-West Spain). Sci. Total Environ. 227 (1), 73–83.

Elbaz-Poulichet, F., Braungardt, C., Achterberg, E., Morley, N., Cossa, D., Beckers, J.M., Nomerange, P., Cruzado, A., Leblanc, M., 2001a. Metal biogeochemistry in the Tinto–Odiel rivers (Southern Spain) and in the Gulf of Cadiz: a synthesis of the results of TOROS project. Cont. Shelf Res. 21 (18–19), 1961–1973.

Elbaz-Poulichet, F., Guieu, C., Morley, N., 2001b. A reassessment of trace metal budgets in the western Mediterranean Sea. Mar. Pollut. Bull. 42 (8), 623–627.

Falkowski, P.G., Barber, R.T., Smetacek, V., 1998. Biogeochemical controls and feedbacks on ocean primary production. Science 281, 200–206.

Gerringa, L.J.A., Veldhuis, M.J.W., Timmermans, K.R., Sarthou, G., de Baar, H.J.W., 2006. Co-variance of dissolved Fe-binding ligands with biological observations in the Canary Basin. Mar. Chem. 102, 276–290.

Gledhill, M., van den Berg, C.M.G., 1994. Determination of complexation of iron(III) with natural organic complexing ligands in seawater using cathodic stripping voltammetry. Mar. Chem. 47, 41–54.

Gomez, F., 2003. The role of exchanges through the Strait of Gibraltar on the budget of elements in the Western Mediterranean Sea: consequences of human-induced modifications. Mar. Pollut. Bull. 40, 685–694.

Gomez, F., Gonzalez, N., Echevarria, F., Garcia, C.M., 2000. Distribution and fluxes of dissolved nutrients in the Strait of Gibraltar and its relationships to microphytoplankton biomass. Estuar., Coast. Shelf Sci. 51 (4), 439–449.

Gong, S.L., Zhang, X.Y., Zhao, T.L., Barrie, L.A., 2004. Sensitivity of Asian dust storm to natural and anthropogenic factors. Geophys. Res. Lett. 31, L07210. doi:10.1029/2004GL019502.

Grasshoff, K., 1983. Automated chemical analysis. In: Grasshoff, K., Ernhardt, M., Kremling, K. (Eds.), Methods of Seawater Analysis. Verlag, pp. 263–289.

Guieu, C., Chester, R., Nimmo, M., Martin, J.-M., Guerzoni, S., Nicolas, E., Mateu, J., Keyse, S., 1997. Atmospheric inputs of dissolved and particulate metals to the Northwestern Mediterranean. Deep-Sea Res. 44 (3–4), 655–674.

Guieu, C., Bozec, Y., Blain, S., Ridame, C., Sarthou, G., Leblond, N., 2002. Impact of high Saharan dust inputs on dissolved iron concentrations in the Mediterranean Sea. Geophys. Res. Lett. 29 (19), 1911. doi:10.1029/2001GL014454.

Hall, R.J., Likens, G.E., Fiance, S.B., Hendrey, G.R., 1980. Experimental acidification of a stream in the Hubbarb Brook Experimental Forest, New Hampshire. Ecology 61 (4), 976–989.

Hernandez-Guerra, A., Fraile-Nuez, E., Lopez-Laatzen, F., Martinez, A., Parrilla, G., Velez-Belchi, P., 2005. Canary current and North Equatorial current from an inverse box model. J. Geophys. Res. 110, C12019. doi:10.1029/2005JC003032.

Hutchins, D.A., DiTullio, G.R., Bruland, K.W., 1993. Iron and regenerated production: evidence for biological iron recycling in two marine environments. Limnol. Oceanogr. 38 (6), 1242–1255.

Hutchins, D.A., Witter, A.E., Butler, A., Luther III, G.W., 1999. Competition among marine phytoplankton for different chelated iron species. Nature 400, 858–861.

Hutchins, D.A., Hare, C.E., Weaver, R.S., Zhang, Y., Firme, G.F., Ditullio, G.R., Aim, M.B., Riseman, S.F., Maucher, J.M., Geesey, M.E., Trick, C.G., Smith, G.J., Rue, E.L., Conn, J., Bruland, K.W., 2002. Phytoplankton iron limitation in the Humboldt Current and Peru Upwelling. Limnol. Oceanography 47 (4), 997–1011.

Jickells, T., 1999. The inputs of dust derived elements to the Sargasso Sea: a synthesis. Mar. Chem. 68, 5–14.

Jickells, T.D., An, Z.S., Andersen, K.K., Baker, A.R., Bergametti, G., Brooks, N., Cao, J.J., Boyd, P.W., Duce, R.A., Hunter, K.A., Kawahata, H., Kubilay, N., La Roche, J., Liss, P.S., Mahowald, N., Prospero, J.M., Ridgwell, A.J., Tegen, I., Torres, R., 2005. Global iron connections between desert dust, ocean biogeochemistry, and climate. Science 308, 67–71.

Johnson, K.S., Gordon, R.M., Coale, K.H., 1997. What controls dissolved iron concentrations in the world ocean? Mar. Chem. 57, 137–161.

Johnson, K.S., Elrod, V.A., Fitzwater, S.E., Plant, J.N., Chavez, F.P., Tanner, S.J., Gordon, R.M., Westphal, D.L., Perry, K.D., Wu, J.F., Karl, D.M., 2003. Surface ocean-lower atmosphere interactions in the Northeast Pacific Ocean Gyre: aerosols, iron, and the ecosystem response— art. no. 1063. Glob. Biogeochem. Cycles 17 (2), 54–69.

Kramer, J., Laan, P., Sarthou, G., Timmermans, K.R., de Baar, H.J.W., 2004. Distribution of aluminium in the high atmospheric input region of the subtropical waters of the North Atlantic Ocean. Mar. Chem. 88 (3–4), 85–101.

Kuma, K., Tanaka, J., Matsunaga, K., Matsunaga, K., 2000. Effect of hydroxamate ferrisiderophore complex (ferrichrome) on iron uptake and growth of a coastal marine diatom, *Chaetoceros sociale*. Limnol. Oceanogr. 45 (6), 1235–1244.

Laës, A., Blain, S., Laan, P., Achterberg, E.P., Sarthou, G., de Baar, H.J.W., 2003. Deep dissolved iron profiles in the eastern North Atlantic in relation to water masses. Geophys. Res. Lett. 30 (17), 1902. doi:10.1029/2003GL017902.

Liu, X., Millero, F.J., 2002. The solubility of iron in seawater. Mar. Chem. 77 (1), 43–54.

Löscher, B.M., de Baar, H.J.W., de Jong, J.T.M., Veth, C., Dehairs, F., 1997. The distribution of Fe in the Antarctic circumpolar current. Deep-Sea Res., Part 2, Top. Stud. Oceanogr. 44, 143–187.

Mahowald, N., Kohfeld, K., Hansson, M., Balkanski, Y., Harrison, S.P., Prentice, I.C., Schulz, M., Rodhe, H., 1999. Dust sources and deposition during the last glacial maximum and current climate: a comparison of model results with paleodata from ice cores and marine sediments. J. Geophys. Res. 104, 15895–15916.

Mahowald, N.M., Baker, A.R., Bergametti, G., Brooks, N., Duce, R.A., Jickells, T.D., Kubilay, N., Prospero, J.M., Tegen, I., 2005. Atmospheric global dust cycle and iron inputs to the ocean. Glob. Biogeochem. Cycles 19, GB4025. doi:10.1029/2004GB002402.

Martin, J.H., Fitzwater, S.E., Gordon, R.M., Hunter, C.N., Tanner, S.J., 1993. Iron, primary production and carbon-nitrogen flux studies during the JGOFS North Atlantic Bloom Experiment. Deep-Sea Res. 40 (1/2), 115–134.

Martin, J.H., Coale, K.H., Johnson, K.S., Fitzwater, S.E., Gordon, R.M., Tanner, S.J., Hunter, C.N., Elrod, V.A., Nowiicki, J.L., Coley, T.L., Barber, R.T., Lindley, S., Watson, A.J., Van Scoy, K., Law, C.S., Liddicoat, M.I., Ling, R., Stanton, T., Stockel, J., Collins, C., Anderson, A., Bidigare, R., Ondrusek, M., Latasa, M., Millero, F.J., Lee, K., Yao, W., Zhang, J.Z., Friederich, G., Sakamoto, C., Chavez, F., Buck, K., Kolber, Z., Greene, R., Falkowski, P., Chisholm, S.W., Hoge, F., Swift, R., Yungel, J., Turner, S., Nightingale, P., Hatton, A., Liss, P., Tindale, N.W., 1994. Testing the iron hypothesis in ecosystems of the equatorial Pacific Ocean. Nature 371, 123–129.

Mazé, J., Arhan, M., Mercier, H., 1997. Volume budget of the eastern boundary layer off the Iberian Peninsula. Deep-Sea Res., Part 1, Oceanogr. Res. Pap. 44, 1543–1574.

Measures, C.I., Brown, E.T., 1996. Estimating dust input to the Atlantic Ocean using surface water Al concentrations. In: Guerzoni, Chester (Eds.), The Impact of African Dust Across the Mediterranean. Kluwer, p. 389.

Measures, C.I., Grant, B., Khadem, M., Lee, D.S., Edmond, J.M., 1984. Distribution of Be, Al, Se and Bi in the surface water of the Western North Atlantic and Carribean. Earth Planet. Sci. Lett. 71, 1–12.

Measures, C.I., Brown, M.T., Vink, S., 2005. Dust deposition to the surface waters of the western and central North Pacific inferred from surface water dissolved aluminum concentrations. Geochem. Geophys. Geosyst. 6, Q09M03. doi:10.1029/2005GC000922.

Millero, F.J., 1998. Solubility of Fe(III) in seawater. Earth Planet. Sci Lett. 154, 323–329.

Mittelstaedt, E., 1991. The ocean boundary along the northwest African coast: circulation and oceanographic properties at the sea surface. Prog. Oceanogr. 26, 307–355.

Morel, F.M.M., Price, N.M., 2003. The biogeochemical cycles of trace metals in the Oceans. Science 300 (5621), 944–947. doi:10.1126/science.1083545.

Morley, N.H., Burton, J.D., Tankere, S.P.C., Martin, J.-M., 1997. Distribution and behaviour of some dissolved trace metals in the western Mediterranean Sea. Deep-Sea Res. 44 (II), 675–691.

Obata, H., Karatani, H., Nakayama, E., 1993. Automated determination of iron in seawater by chelating resin concentration and chemiluminescence. Anal. Chem. 65, 1524–1528.

Parekh, P., Follows, M.J., Boyle, E.A., 2005. Decoupling of iron and phosphate in the global ocean. Glob. Biogeochem. Cycles 19, GB2020. doi:10.1029/2004GB002280.

Pérez-Marrero, J.O., Llinas, L.M., Rueda, M.J., Cianca, A., 2002. Saharan dust storms over the Canary Islands during winter 1998 as depicted from the advanced very high-resolution radiometer. Deep-Sea Res., Part 2, Top. Stud. Oceanogr. 49 (17), 3465–3479.

Prospero, J.M., 1996. Saharan dust transport over the North Atlantic Ocean and Mediterranean: an overview. In: Guerzoni, S., Chester, R. (Eds.), The Impact of Desert Dust Across the Mediterranean. Kluwer, Dordrecht, pp. 133–151.

Prospero, J.M., Ginoux, P., Torres, O., Nicholson, S.E., Gill, T.E., 2002. Environmental characterization of global sources of atmospheric soil dust identified with the NIMBUS 7 Total Ozone Mapping Spectrometer (TOMS) absorbing aerosol product. Rev. Geophys. 40 (1), 1002. doi:10.1029/2000RG000095.

Ratmeyer, V., Fischer, G., Wefer, G., 1999. Lithogenic particle fluxes and grain size distributions in the deep ocean off northwest Africa: implications for seasonal changes of aeolian dust input and downward transport. Deep-Sea Res., Part 1, Oceanogr. Res. Pap. 46, 1289–1337.

Richardson, P.L., 1993. Tracking ocean eddies. Am. Sci. 81, 261–271.

Richardson, P., Walsh, S., Armi, L., Schröder, M., Price, J., 1989. Tracking three meddies with SOFAR floats. J. Phys. Oceanogr. 19, 371–383.

Ridame, C., Guieu, C., Loye-Pilot, M.D., 1999. Trend in total atmospheric deposition fluxes of aluminium, iron and trace metals in the northwestern Mediterranean over the past decade (1985–1997). J. Geophys. Res. 104 (D23), 127–138.

Rose, A.L., Salmon, T.P., Lukondeh, T., Neilan, B.A., Waite, T.D., 2005. Use of superoxide as an electron shuttle for iron acquisition by the marine cyanobacterium *Lyngbya majuscula*. Environ. Sci. Technol. 39 (10), 3708–3715. doi:10.1021/es048766cS0013-936X(04)08766-8.

Rossby, T., 1988. Five drifters in a Mediterranean salt lens. Deep-Sea Res., Part 1, Oceanogr. Res. Pap. 35, 1653–1663.

Rue, E.L., Bruland, K.W., 1995. Complexation of iron(III) by natural organic ligands in the Central North Pacific as determined by a new competitive ligand equilibration/adsorptive cathodic stripping voltammetric method. Mar. Chem. 50 (1–4), 117–138.

Rue, E.L., Bruland, K.W., 1997. The role of organic complexation on ambient iron chemistry in the equatorial Pacific Ocean and the response of a mesoscale iron addition experiment. Limnol. Oceanogr. 42 (5), 901–910.

Santana-Casiano, J.M., Gonzalez-Davila, M., Rodriguez, M.J., Millero, F.J., 2000. The effect of organic compounds in the oxidation kinetics of Fe(II). Mar. Chem. 70, 211–222.

Sarthou, G., Jeandel, C., 2001. Seasonal variations of iron concentrations in the Ligurian Sea and iron budget in the Western Mediterranean Sea. Mar. Chem. 74 (2–3), 115–129.

Sarthou, G., Baker, A.R., Blain, S., Achterberg, E.P., Boye, M., Bowie, A.R., Croot, P.L., Laan, P., de Baar, H.J.W., Jickells, T.D., Worsfold, P.J., 2003. Atmospheric iron deposition and sea-surface dissolved iron concentrations in the eastern Atlantic Ocean. Deep-Sea Res., Part 1, Oceanogr. Res. Pap. 50 (10–11), 1339–1352.

Sedwick, P.N., Church, T.M., Bowie, A.R., Marsay, C.M., Ussher, S.J., Achilles, K.M., Lethaby, P.J., Johnson, R.J., Sarin, M.M., McGillicuddy, D.J., 2005. Iron in the Sargasso Sea (Bermuda Atlantic Time-series Study region) during summer: eolian imprint, spatiotemporal variability, and ecological implications. Glob. Biogeochem. Cycles 19 (4), 14–26. doi:10.1029/2004GB002445 (GB4006).

Swap, R., Ulanski, S., Cobbett, M., Garstand, M., 1996. Temporal and spatial characteristtics of Saharan dust outbreaks. J. Geophys. Res. 101, 4205–4220.

Taylor, S.R., McLennan, S.M., 1985. The Continental Crust: Its Composition and Evolution. Blackwell, Oxford, 312 pp.

Tegen, I., Fung, I.Y., 1994. Modeling of mineral dust in the atmosphere: sources, transport and optical thickness. J. Geophys. Res. 99, 2897–2914.

Torres-Padron, M.E., Gelado-Caballero, M.D., Collado-Sanchez, C., Siruela-Matos, V.F., Cardona-Castellano, P.J., Hernandez-Brito, J.J., 2002. Variability of dust inputs to the CANIGO zone. Deep-Sea Res., Part 2, Top. Stud. Oceanogr. 49 (17), 3455–3464.

van den Berg, C.M.G., 1995. Evidence for organic complexation of iron in seawater. Mar. Chem. 50 (1–4), 139–156.

van Geen, A., Boyle, E.A., Moore, W.S., 1991. Trace metal enrichments in waters of the Gulf of Cadiz, Spain. Geochim. Cosmochim. Acta 55 (8), 2173–2191.

Veldhuis, M.J.W., Kraay, G.W., 2004. Phytoplankton in the subtropical Atlantic Ocean: towards a better assessment of biomass and composition. Deep-Sea Res., Part 1, Oceanogr. Res. Pap. 51 (4), 507–530.

Veldhuis, M.J.W., Timmermans, K.R., Croot, P., van der Wagt, B., 2005. Picophytoplankton: a comparative study of their biochemical composition and photosynthetic properties. J. Sea Res. 53, 7–24.

Welch, K.D., Davis, T.Z., Aust, S.D., 2002. Iron autoxidation and free radical generation: effects of buffers, ligands, and chelators. Arch. Biochem. Biophys. 397 (2), 360–369.

Wells, M.L., Trick, C.G., 2004. Controlling iron availability to phytoplankton in iron-replete waters. Mar. Chem. 86, 1–13.

Wu, J.F., Boyle, E., 2002. Iron in the Sargasso Sea: implications for the processes controlling dissolved Fe distribution in the ocean. Glob. Biogeochem. Cycles 16 (4), 464–471.

Wu, J., Luther III, G.W., 1994. Size-fractionated iron concentrations in the water column of the Northwest Atlantic Ocean. Limnol. Oceanogr. 39, 1119–1129.

Wu, J., Luther III, G.W., 1995. Complexation of Fe(III) by natural organic ligands in the Northwest Atlantic Ocean by a competitive ligand equilibration method and a kinetic approach. Mar. Chem. 50 (1–4), 159–177.

Wu, J., Boyle, E., Sunda, W., Wen, L.-S., 2001. Soluble and colloidal iron in the oligotrophic North Atlantic and North Pacific. Science 293, 847–849.

Yoon, Y.-Y., Martin, J.-M., Cotte, M.H., 1999. Dissolved trace metals in the Western Mediterranean Sea: total concentration and fraction isolated by C18 Sep-Pak technique. Mar. Chem. 66, 129–148.